Jamming a Drone - EM Simulation of Simple EW and EW Countermeasures Scenarios

Tomislav Milošević

***Abstract*—The paper discusses electromagnetic simulations (EM) of an electronic warfare (EW) scenario where a drone is jammed using a continuous wave (CW) jammer. EW countermeasures have been proposed based on calculated currents induced on specific parts of the drone critical for jamming effectiveness, such is antenna or wire in printed circuit board. All the simulations relate to widely used 2.4 GHz frequency band.**

***Index Terms*—jamming, drone, anti-drone.**

I. Introduction

VARIOUS types of drones exist on a consumer market spanning from pieces dedicated to sport or entertainment to high class devices capable to carry out complex tasks. Besides utilization of drones along with positive legislation, even drones with basic functionality can potentially be used for malicious activities in scenarios which are not socially tolerable or could even be harmful. For example, a very basic drone can be used by paparazzi in invading celebrities' privacy or by criminals and terrorists in compromising security of a potential target. Therefore, in parallel with development of the drones, various anti-drone systems have been developed as well.

This paper presents a scenario where a radio-controlled drone is flying within an active zone of an anti-drone system. Anti-drone system itself is simply a helix antenna with a reflector.

Communication systems in general may exhibit restricted or completely inhibited functionality when subjected to interference, jamming or outer EW measures [1], [2]. Described model of jamming system represents the class of anti-drone systems which uses a CW signal to jam the drone flight-control receiver. In order to reduce the effect of the jammer, simple passive countermeasures can be used. In general, passive countermeasures do not involve the emission of any signals or noise [1]. It will be shown that using the results of EM reconnaissance, a simple, partial shielding of the jamming sensitive parts of the drone can significantly reduce the effectiveness of the jamming. It is assumed that anti-drone system and the drone receiver both operate at 2.4 GHz, the frequency widely used for Wireless LAN [3].

The basic principle of an anti-drone system operation is to induce current – a strong jamming signal on the drone side and saturate the receiver. Also, it is possible that the anti-drone system induces current in the printed circuit board (PCB) which is a part of the drone electronic system causing the malfunctioning of onboard electronics. Addressing the practical side of anti-drone system as described, one can say that receiving of control signals through the drone receiver will be blocked and that additionally a spurious signal would be induced in the electronic circuits.

The effects of the jamming will be simulated using WIPL-D Pro, a full wave 3D electromagnetic Method-of-Moments (MoM) based software which applies Higher Order Basis Functions over bilinear surfaces combined with Surface Integral Equations [4]. The software considers the bilinear surfaces as nonplanar quadrilaterals defined uniquely by four vertices [5]. Thanks to the inherent property of MoM, the size of EM model and accordingly the complexity of the simulation does not increase with increased jammer-to-drone distance [4].

II. Model of the Drone

The model of the drone is shown in the Fig. 1. It contains a camera mounted below the drone, which represents a payload of the drone. The drone with its payload is modeled as a dielectric object with the following dielectric properties: ε_{rReal}=2.2 and ε_{rImag}=-0.066. Beside the dielectric, the drone contains some metallic parts which are also shown in the Fig. 1. The "upper" metallic parts represent the monopole antenna with the ground plane. The monopole antenna is intended to be used for receiving flight control signals. The "lower" metallic parts represent a simplified PCB with a rectangular half-loop on it.

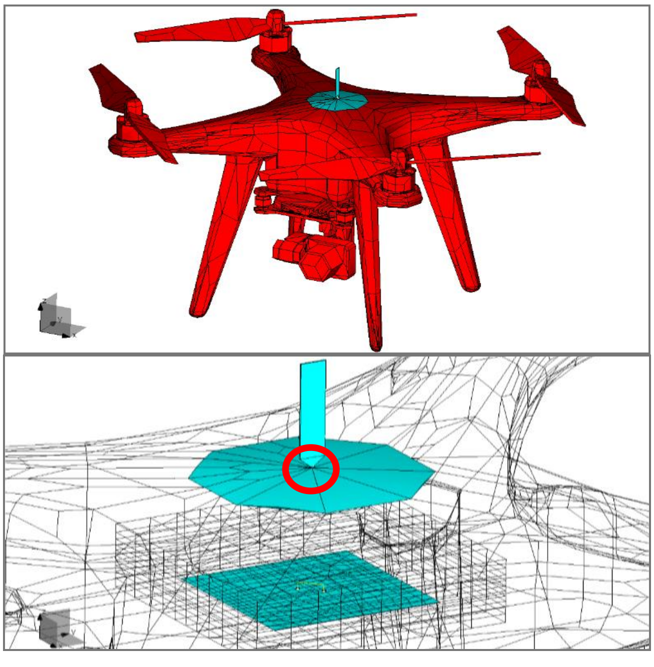

Figure 1. The model of the drone with the payload and the metallic parts of the drone.

Tomislav Milošević is with WIPL-D d.o.o., Gandijeva 7, 11073 Belgrade, Serbia (e-mail: tomislav.milosevic@wipl-d.com).

Inducing the jamming current on the receiver will be monitored on the wire used to feed the monopole antenna. The wire is located at the very end of the antenna and it is encircled in red in Fig. 1.

The current induced in drone PCB is monitored on the grounded half-loop. Actually, as presented with markings outlined in the Fig. 2, the induced current is calculated over the "horizontal" wire. The dimensions of the metallic surface representing demonstration model of the PCB and the half-loop are also displayed in the Fig. 2.

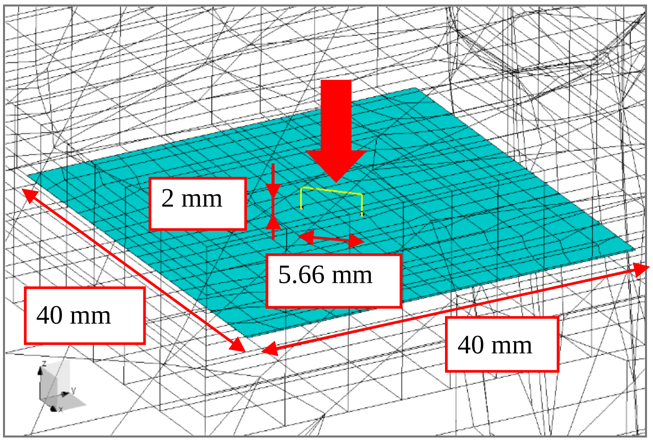

Figure 2. Demonstration model of the circuit board located within the drone.

It can be seen in the Fig. 3 that interior of the drone accommodates the described model of a PCB where onboard electronics is located. In other words, the metallic surface and the half-loop are immersed in the air box inside the drone dielectric.

The S-parameters and 3D radiation pattern[1] of the monopole antenna from Fig. 1 when the drone hovers above the PEC plane are shown in the Fig. 4.

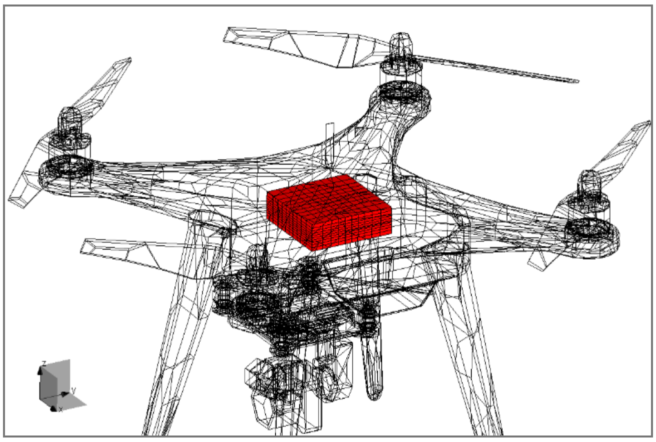

Figure 3. The air box in which the PCB with the half-loop is located.

III. The Model of the Jammer

The simplified model of the jammer in the form of the EM gun only contains a helix antenna and an octagon reflector both located over the PEC ground plane. The details related to geometry of the EM gun structure are presented in the Fig. 5. The center of the antenna reflector is located at the height of 0.1 meter and the axis of the helix is oriented at elevation angle of 35°. The radiation pattern of the jammer antenna above PEC plane is also shown in the Fig. 5. It can be seen that the 3D radiation pattern is influenced by PEC presence and that the position of the antenna has been adjusted to boost the radiation at a sector of interest to a gain higher than 10 dB. The sector of interest covers elevation angles from approximately 9° to approximately 57°.

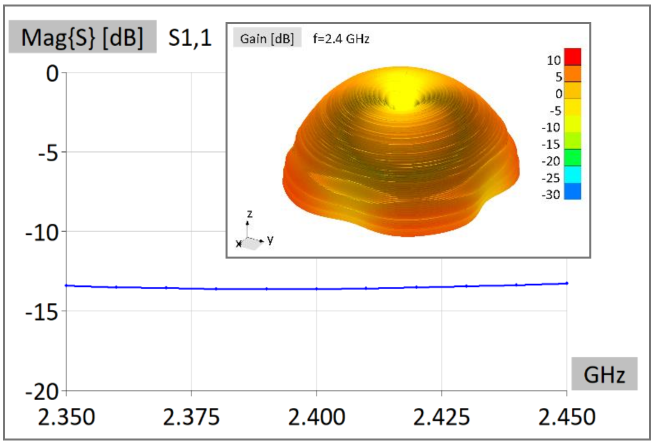

Figure 4. S-parameters and radiation pattern of the monopole mounted on the drone hovering above PEC plane.

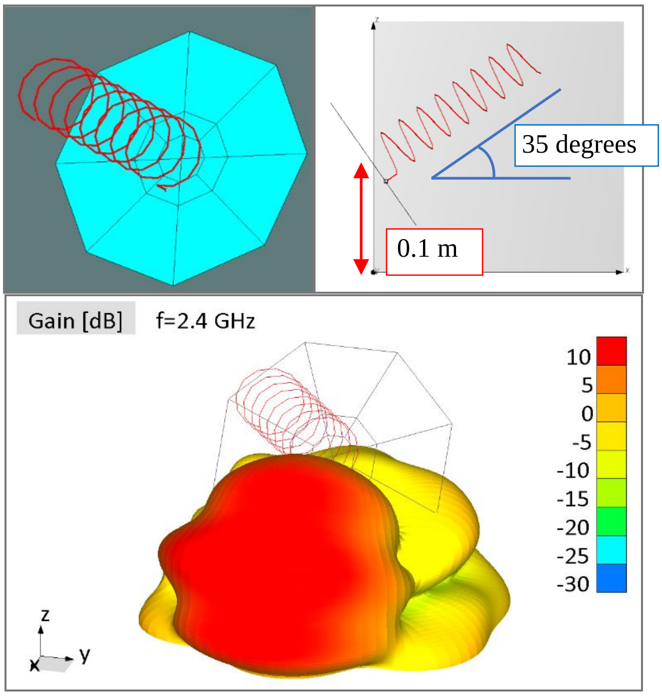

Figure 5. The model and the position of the jammer/EM gun over the PEC plane with 3D radiation pattern at 2.4 GHz.

IV. Jamming Scenario

The particular jamming scenario is illustrated in the Fig. 6 in 3D view, bird's view, and side view, from top to bottom. Both, drone and anti-drone system are located above the ground modeled as a Perfect Electric Conductor (PEC) plane. It is assumed that the drone flies through the zone protected with the jammer along a straight line, which is a realistic assumption.

[1] In this paper, all *Gain* values are in dBi.

The top part of the Fig. 6 shows the direction of the antenna rotation starting from the lowest phi angle (phi = 0°) and the drone flight direction. The middle part of the figure explains the details related to the distance between the antenna and the drone, the angles of antenna rotation, and the drone flight direction. Finally, the lower part of the figure shows the side view of the jamming scenario.

The initial location of the drone is (x, y, z) = (15 m, 0 m, 5 m). The final location of the drone is (x, y, z) = (15 m, 25.98 m, 5 m). The jammer antenna is located in (x, y, z) = (0 m, 0 m, 0.1 m) as shown in Fig. 6 and it is being rotated from phi=0° to phi=60° (Fig. 6) keeping the elevation angle of 35°. This means that the monopole antenna mounted on the drone is constantly illuminated with the jammer signal during the described flight along the straight line. The helix antenna which is part of the jammer operates in axial mode at 2.4 GHz (see also Fig. 4 and S_{11} of the monopole antenna mounted on the drone).

Induced current in the middle of the wire located in the root of the monopole antenna mounted on the drone is shown in the Fig. 7. The current induced in the middle of the wire which is part of the half-loop on the PCB is shown in the Fig. 8.

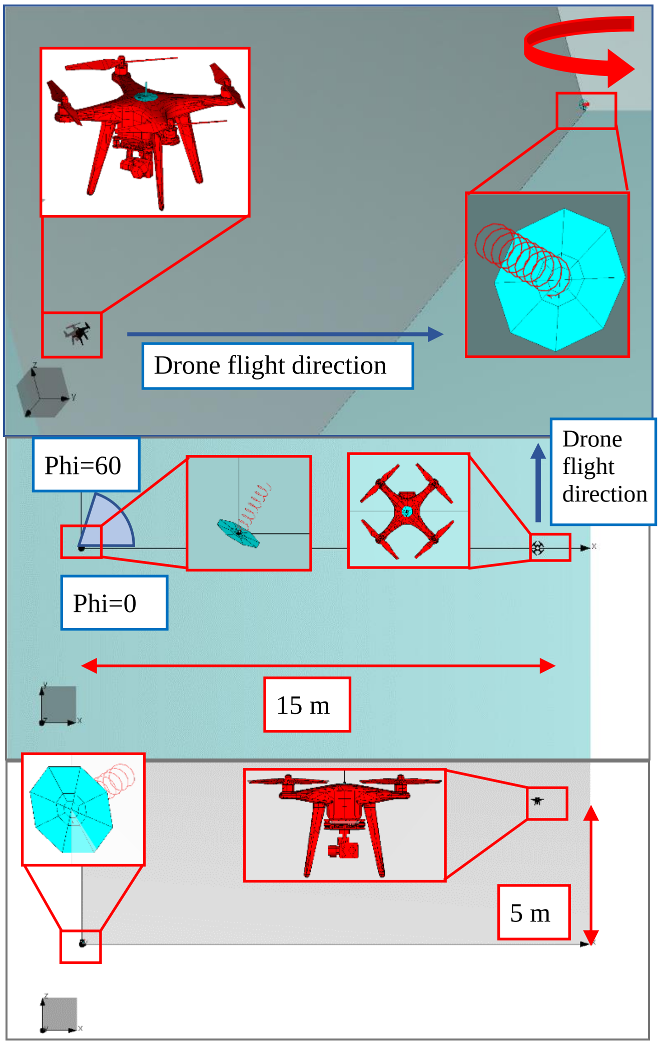

Figure 6. Investigated scenario in 3D, birds view, and side view, from top to bottom, respectively.

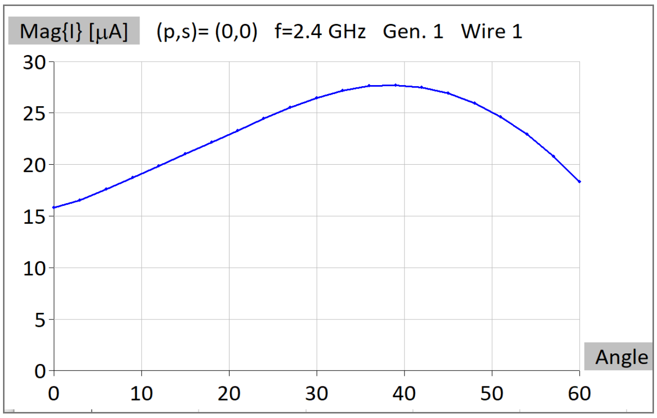

Figure 7. The current induced in the middle of the wire in the root of the monopole antenna.

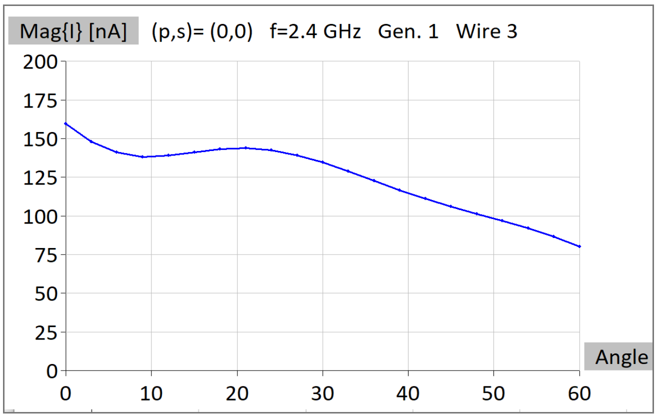

Figure 8. The current induced in the middle of the upper wire in the half-loop on PCB.

V. Decreasing Jamming Effectiveness

The presumption of the successful jammer countermeasures is the reliable information of the exact position of the jammer which can be revealed by visual surveillance or EM reconnaissance.

In order to decrease jamming effectiveness, the drone can be modified using a simple, commonly available objects. The PBC area can be easily protected from the outer influence by enclosing it in full (could be a piece of food-wrapping aluminum foil), which is a straight-forward action. However, the antenna used for receiving control signals cannot be fully enclosed for obvious reasons, but, when the position of the jammer is known, it can be partially enclosed so that the covered part coincides with the direction where the jammer is located. The very simple enclosure will be considered here, the one comprising a smooth cylinder or conical object (could be a disposable paper cup). with a metalized part located towards the jammer as described (again, the metallization could simply be a piece of an aluminum foil).

The model of the modified drone is shown in the Fig. 9. The drone dielectric is being displayed in yellow in the upper part of this figure. The cup, with assumed relative dielectric constant of $\varepsilon_{rCupReal}=3$ is colored in blue. The metallic sheet representing the aluminum foil is in cyan and clearly visible in both parts of the Fig. 9. Mechanical connections which should be added to real-life drone structure are excluded from this EM model, without losing the quality of approximation. Enclosing the PCB using thin metal sheet following a box shape displayed in Fig. 3 can be noticed in the lower part of the Fig. 9. More precise explanation of the scenario with metallic sheet is presented in Fig. 10 where the arrow points to the cup which is mounted on the top of the drone. In other words, the metallic sheet is positioned on the left side of the cup.

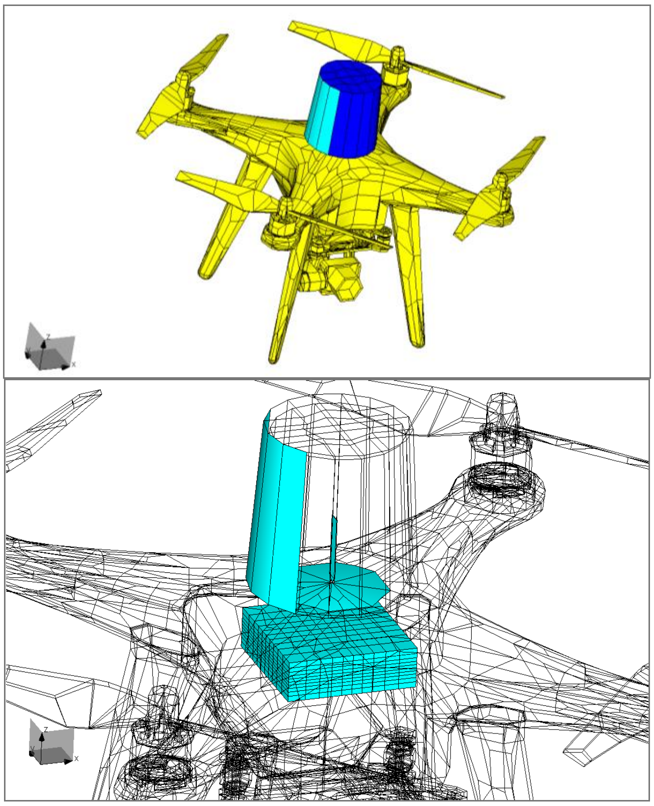

Figure 9. The drone with modifications and the metallic parts with enclosing of PCB.

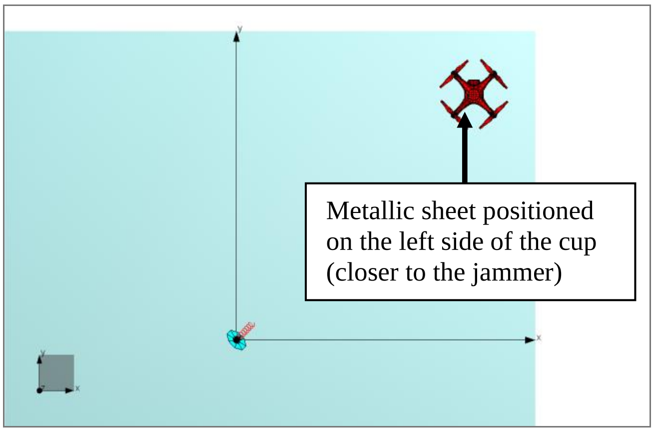

Figure 10. The position of the drone and the jammer with explained position of the metallic sheet. Not to be scaled.

The output results are displayed and compared in Figs 11-12. Fig. 11 displays comparison of the induced currents on the wire in the root of the antenna without the cup, with the cup and metallic sheet, and with the metallic sheet, only. It can be seen that without the metallic sheet attached to the cup, the level of induced current is the highest. Adding metallic sheet wrapped around the cup lower levels of induced currents are obtained. Similar result appears with the metallic sheet added and without the cup. This proves that metallic sheet mainly influences the jamming signal.

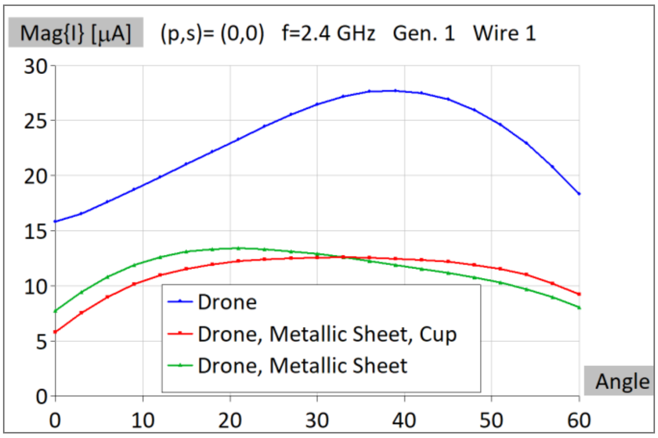

Figure 11. The comparison of currents induced in the middle of the wire in the root of the monopole antenna.

Fig. 12 displays comparison of currents on the PCB wire in three previously explained cases. The drop in level of the induced signal for shielded PCB is clearly noticeable.

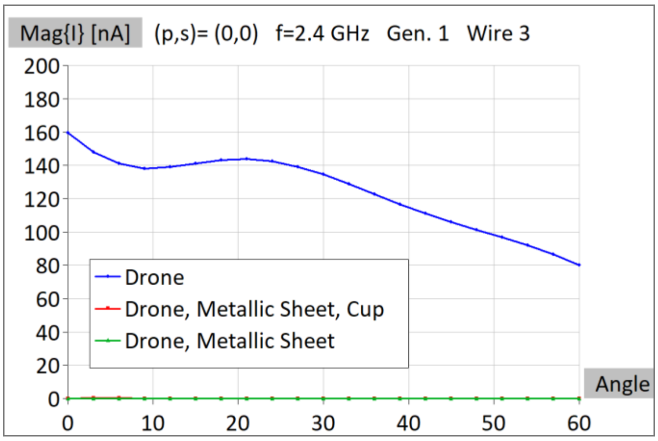

Figure 12. The comparison of currents induced in the middle of the upper wire in the half-loop on PCB

VI. Computer Platform and Simulation Time

All scenarios were simulated using a MoM based software and dedicated sweeping tool rotating the jammer from angle phi=0° to phi=60° in 21 equidistant points and moving the drone in the appropriate direction. The most demanding simulation of the jammed drone with the metallic sheet and the cup required 16,761 elements and 36,060 unknowns. The simulation time per a single angle of rotation for the same model is about than 8 minutes. The computer used for carrying out the simulation is Intel® Xeon® Gold 5118 CPU @ 2.30GHz (2 processors) with 192 GB RAM and a GPU card NVIDIA GeForce GTX 1080 Ti. GPU card is used for both matrix fill-in and matrix inversion.

VII. Conclusion

A scenario encompassing the drone and an anti-drone system in the form of an EM gun over the PEC ground plane has been investigated. The effectiveness of jamming is demonstrated by calculating the induced currents at 2.4 GHz. Also, basic countermeasures were presented based on simple modifications of the drone.

The main effect of the jamming comes from the saturation of the receiver. Such a result can be explained easily as the antenna is directly exposed to the jamming signal. It was shown that mounting metallic sheet between the jammer and the receiving monopole, using an auxiliary cylindrical object like a paper cup, can significantly reduce the effectiveness of the jammer signal.

The current induced in the PCB elements might cause malfunction of drone electronics but being significantly lower than the level of the current on the antenna connection, is of secondary importance to the jamming scenario. Furthermore, the countermeasures can be performed easier by enclosing critical area around the PCB.

As it has been confirmed that simple countermeasures can make the drone resilient to jamming from a single source, the counter-countermeasures should include the distribution of several jammers in different locations around the target as it makes the method of partial shielding impractical.

Utilization of a Method-of-Moments (MoM) based software, for calculation of the induced currents has been also demonstrated. The numerical results have been obtained with high efficiency on an affordable desktop machine.

Further investigation could include propagation effects, or adding some objects such as metallic fences or lampposts and their influence on jammer-to-drone link.

References

[1] D. M. Pozar, Microwave Engineering, 2nd ed., USA, John Wiley & Sons, 1998.

[2] D. Banjac, Electronic Warfare in Anti-Aircraft Defense (in Serbian), Military Publishing and Media Center, Belgrade, 1986.

[3] J. L. Volakis, Antenna Engineering Handbook, 4th ed., USA: McGraw-Hill, 2007

[4] WIPL-D Software, WIPL-D d.o.o, Belgrade 2021. www.wipl-d.com

[5] B. M. Kolundzija, A. R. Djordjevic, Electromagnetic Modeling of Composite Metallic and Dielectric Structures, 1st ed. Norwood, Massachusetts, USA: Artech House, 2002.